Distribution of Corneal TRPV1 and Its Association With Immune Cells During Homeostasis and Injury

Haihan Jiao,[1,2] Jason J. Ivanusic,[2] Paul G. McMenamin,[3] and Holly R. Chinnery[1]

[1]Department of Optometry and Vision Sciences, University of Melbourne, Parkville, Australia
[2]Department of Anatomy and Physiology, University of Melbourne, Parkville, Australia
[3]Department of Anatomy & Developmental Biology, Faculty of Medicine, Nursing and Health Sciences, Monash University, Clayton, Australia

Correspondence: Holly R. Chinnery, Department of Optometry and Vision Sciences, Faculty of Medicine, Dentistry & Health Sciences, The University of Melbourne, Parkville VIC 3010, Australia; holly.chinnery@unimelb.edu.au.

Received: October 24, 2020
Accepted: May 31, 2021
Published: July 7, 2021

Citation: Jiao H, Ivanusic JJ, McMenamin PG, Chinnery HR. Distribution of corneal TRPV1 and its association with immune cells during homeostasis and injury. *Invest Ophthalmol Vis Sci.* 2021;62(9):6. https://doi.org/10.1167/iovs.62.9.6

Purpose. Given the role of corneal sensory nerves during epithelial wound repair, we sought to examine the relationship between immune cells and polymodal nociceptors following corneal injury.

Methods. Young C57BL/6J mice received a 2 mm corneal epithelial injury. One week later, corneal wholemounts were immunostained using β-tubulin-488, TRPV1 (transient receptor potential ion channel subfamily V member-1, a nonselective cation channel) and immune cell (MHC-II, CD45 and CD68) antibodies. The sum length of $TRPV1^+$ and $TRPV1^-$ nerve fibers, and their spatial association with immune cells, was quantified in intact and injured corneas.

Results. $TRPV1^+$ nerves account for ~40% of the nerve fiber length in the intact corneal epithelium and ~80% in the stroma. In the superficial epithelial layers, $TRPV1^+$ nerve terminal length was similar in injured and intact corneas. In intact corneas, the density (sum length) of basal epithelial $TRPV1^+$ and $TRPV1^-$ nerve fibers was similar, however, in injured corneas, $TRPV1^+$ nerve density was higher compared to $TRPV1^-$ nerves. The degree of physical association between $TRPV1^+$ nerves and intraepithelial $CD45^+$ $MHC\text{-}II^+$ $CD11c^+$ cells was similar in intact and injured corneas. Stromal leukocytes co-expressed TRPV1, which was partially localized to $CD68^+$ lysosomes, and this expression pattern was lower in injured corneas.

Conclusions. $TRPV1^+$ nerves accounted for a higher proportion of corneal nerves after injury, which may provide insights into the pathophysiology of neuropathic pain following corneal trauma. The close interactions of $TRPV1^+$ nerves with intraepithelial immune cells and expression of TRPV1 by stromal macrophages provide evidence of neuroimmune interactions in the cornea.

Keywords: cornea, neuroimmune, nociceptors, TRPV1

Corneal sensory nerves, which are critical in maintaining corneal integrity, can be divided into three main functional subtypes of nociceptive terminals located in the epithelium: polymodal nociceptors, pure mechanonociceptors, and cold-sensing thermoreceptors (reviewed in [1,2]). Stimulation of nociceptors produces acute or persistent pain derived from mechanical, chemical, and thermal stimuli. Polymodal nociceptors are known to contribute to physiological[3] and pathological conditions of the ocular surface,[4] including pain sensation,[5] cold nociception,[6] stromal fibrosis,[7–9] wound healing,[10,11] and corneal neovascularization.[9,12,13] Transient receptor potential ion channel subfamily V member 1 (TRPV1) is a nonselective cation channel that is critical to the function of polymodal nociceptors.[14] It is expressed by polymodal nociceptors in the corneal epithelium, and so is an ideal marker for this subpopulation of corneal sensory neurons.[15] The topographical distribution of $TRPV1^+$ polymodal nociceptors is well described in the corneas of guinea pigs[15,16] and rats.[17–20] In a study comparing the chronic effect of diabetes and high fat diet on the distribution and density of TRPV1 and TRP subfamily M member 8 $(TRPM8)^+$ nerves in the mouse cornea, there was a significant reduction in the proportion of $TRPM8^+$ nerves, whereas $TRPV1^+$ nerves were less affected by the metabolic disturbance.[21] These findings suggest that subpopulations of corneal nerves (i.e., $TRPV1^+$ polymodal nociceptors and the cold-sensing $TRPM8^+$ thermoreceptors) can be differentially affected by neuropathological conditions. In the context of corneal epithelial injury,[22] He et al. (2018) reported the slower recovery of $TRPM8^+$ sensory nerves, which contribute to cold sensing[6] and tear production,[23] compared to substance P-expressing corneal nerves up to 15 weeks postinjury. However, the relative rate of recovery of $TRPV1^+$ nerve fibers was not examined.

Neuroimmune interplay between nociceptors and resident immune cells are paramount in regulating host defense of peripheral tissues, such as skin, gut, and lung. Anatomical and functional studies have reported local dendritic cells (DCs) in physical proximity with nociceptors in murine

skin[24] and lung mucosa.[25] TRPV1$^+$ nociceptors elicit DC cytokine production in pathological conditions of the skin such as psoriasis[26] fungal infection.[27] Local macrophages are spatially associated with peripheral nerve fibers,[28] phagocytose myelin debris,[29–31] and have also been shown to interact with TRPV1$^+$ nociceptors in skin and pancreas to modulate inflammatory macrophage recruitment[32–34] and phagocytosis of microbial pathogens.[35]

The cornea contains resident DCs in the epithelium and macrophages in the stroma that contribute to host defense of the ocular surface. Emerging anatomical evidence has shown the physical proximity of corneal immune cells with intraepithelial nerve fibers[36] and with large limbal nerve trunks in the stroma.[37] Pharmacological depletion of DCs lowers the intraepithelial nerve fiber density.[36] This interdependence of corneal nerves and DCs is facilitated by DC-mediated production of ciliary neurotrophic factor, which enhances nerve regeneration after epithelial injury.[38]

While the studies detailed above clearly demonstrate the existence of TRPV1$^+$ nerves in the mouse cornea, their anatomical distribution and their relationships with the local immune cells during homeostasis and injury remains uncharacterized. In this study we demonstrated a close physical proximity exists between TRPV1$^+$ nerves and resident immune cells, and report punctate intracellular TRPV1 expression within stromal macrophages. This anatomical nociceptor-immune axis may be involved in corneal pain responses following injury at the ocular surface.

Methods

Animals

Male and female C57BL/6J mice at eight to nine weeks of age (n = 7 per group), were purchased from the Animal Resources Centre (Canning Vale, Western Australia) and housed under specific pathogen-free conditions at the Florey Institute of Neuroscience and Mental Health. CD11c-eYFP Crb1$^{wt/wt}$ mice which express eYFP under the control of the *Itgax* promoter (9–10 weeks old), were used to confirm CD11c expression on intraepithelial DCs. Eyes from TRPV1$^{-/-}$ and age-matched wild type mice were kindly gifted by Yuka Okado and Shizuya Saika from Wakayama Medical University, Japan. All animal procedures were approved by the Animal Ethics Committee at the Florey Institute of Neuroscience and Mental Health and complied with the Association for Research in Vision and Ophthalmology (ARVO) Statement for the Use of Animals in Ophthalmic and Vision Research.

Corneal Abrasion

Mice were anesthetized by an intraperitoneal injection of ketamine and xylazine (80 mg/kg and 10 mg/kg; Lyppard, Keysborough, VIC, Australia). To induce the nerve injury, a 2 mm trephine was used to mark the central cornea and the epithelium within this zone was debrided using a corneal rust ring remover (Algerbrush II; Alger Equipment Co., Lago Vista, TX, USA).[39,40] To prevent dryness of the ocular surface, a 2 µL drop of sterile saline was applied. After one week, the mice were euthanized by lethal injection of Lethabarb (100 mg/kg, intraperitoneal; Lyppard, Keysborough, VIC, Australia).

Wholemount Staining

Eyes were fixed in cold 100% methanol for one hour at 4°C and washed in phosphate buffered saline (PBS), three times for five minutes, before corneal dissection. Corneas were permeabilized in 20 mM EDTA for 30 minutes at 37°C and then blocked in PBS containing 3% BSA and 0.3% Triton X-100 for one hour at room temperature. They were then incubated overnight with rabbit α-TRPV1 antibody (1:400, Alomone). Immune cells were immunolabeled by an overnight incubation of rat α-CD45 (1:500, BD Biosciences), rat α- MHC-II (1:400, BD Biosciences), or rat α-CD68 (1:400, AbD Serotec Bio-Rad). Following three PBS washes, corneas were immunolabeled with 488-conjugated βIII-tubulin (1:400, Millipore Merck), washed three times before the incubation with goat anti-rat Cy3 secondary antibodies (1:500, Invitrogen) and Hoechst (1:1000, Sigma-Aldrich) for 1.5 hours at room temperature. The wholemounts were coverslipped with low-fade mounting medium.

To determine the percentage of TRPV1$^+$ nerves in the cornea, double immunostaining was performed by an overnight incubation of α-TRPV1 antibody at 4°C and two hour of goat anti-rabbit-647 secondary antibody. After three PBS washes, corneas were incubated with rabbit anti-β-tubulin-488 conjugated antibody for 1.5 hours at room temperature.

To confirm TRPV1 immunoreactivity, TRPV1 antibody was preadsorbed with the manufacturer's peptide control antigen (Cat #ACC030, Alomone labs) at 0.1 to 1 µg/ml, before immunostaining as above.[41] Eyes from TRPV1 knockout (TRPV1$^{-/-}$) and age-matched wild type (WT) mice were also used to validate the TRPV1 antibody staining.

Confocal Microscopy and Image Analysis

Corneal wholemounts were visualized using a Leica SP8 confocal microscope. Two nonoverlapping confocal z-stacks were collected from central cornea, and three z-stacks from peripheral cornea (area of each image 290 × 290 µm, step size 1 µm),[39] of the double-immunostained βIII TRPV1 wholemounts. Corneal immune cells were imaged under 40× and 63× magnification to examine the relationship of immune cells with TRPV1$^+$ nerve fibers. To assess the DC-nerve contacts in three dimensions, Imaris software was used on higher resolution z-stacks (step size 0.2 µm, 63× magnification). Each corneal image had two to three DCs in the image frame. To examine TRPV1 expression in the stroma, full thickness stromal z-stacks were collected (step size 1 µm). High resolution imaging of macrophage lysosomes (step size 0.3 µm) was performed on CD45$^+$ TRPV1$^+$ and CD68$^+$ TRPV1$^+$ stained corneas using a 63× objective. Huygens deconvolution was performed on the high-resolution confocal z-stacks.

Manual nerve tracing was performed to measure the nerve density (represented as mean sum length per image) of TRPV1$^+$ and TRPV1$^-$ subpopulations in the SNT, SBNP, and stromal nerve plexus using NeuronJ plugin and FIJI as described in previous studies.[39,42] The percentage of TRPV1$^+$ and TRPV1$^-$ nerve fibers in total corneal βIII$^+$ nerve fibers was subsequently calculated for the central and peripheral cornea of intact and injured mice. Analysis of confocal images was masked to avoid bias.

Investigative Ophthalmology & Visual Science

Statistical Analysis

Unpaired Student's *t*-test was performed to report the regional differences in the distribution of TRPV1$^+$ nerve terminals and basal nerve fibers. Two-way ANOVA with Sidak's multiple comparisons were performed to compare the differences between intact and injured corneas. $P < 0.05$ was considered statistically significant. All data expressed as mean ± SEM.

Results

TRPV1$^+$ Nerve Fiber Localization in the Superficial and Basal Epithelium During Steady State

TRPV1$^+$ and TRPV1$^-$ nerve fibers were observed in the superficial nerve terminal (SNT) layer and the subbasal nerve plexus (SBNP) of both the peripheral and the central cornea (Figs. 1A–L). Superficial TRPV1$^+$ nerve fiber density was lower than the TRPV1$^-$ fibers in the central cornea ($P < 0.05$, Fig. 1M) but was similar in the peripheral cornea ($P > 0.05$, Fig. 1M). In the basal epithelium, the sum lengths of TRPV1$^+$ and TRPV1$^-$ SBNP nerve fibers were similar in both the central and peripheral cornea ($P > 0.05$, Fig. 1N).

When considering the proportion of superficially located βIII$^+$ nerves that expressed TRPV1, the peripheral cornea had a significantly higher abundance of TRPV1$^+$ nerves (56% ± 5.1; $n = 7$) than the central cornea (38% ± 5.8) ($P < 0.05$, Fig. 1O). The proportion of TRPV1$^+$ nerves in the SBNP was similar in the central (46% ± 6.8) and peripheral cornea (39% ± 4.3) ($P > 0.05$, Fig. 1P).

TRPV1$^+$ Nerve Fiber Density After Central Epithethial Debridement

We next compared the proportion of βIII$^+$ nerves that expressed TRPV1 one week after a corneal abrasion injury. The proportion of βIII$^+$ TRPV1$^+$ and βIII$^+$ TRPV1$^-$ nerves was different in the central (Figs. 2A–F) and peripheral cornea (Figs. 2G–L). The central cornea exhibited disorganized, complex terminal morphology that appeared to form large islands sprouting from the underlying basal nerves (Fig 2A). The sum length of TRPV1$^+$ SNT was lower than TRPV1$^-$ SNTs in the injured central cornea ($P < 0.05$, Fig. 2M), but similar in the peripheral cornea ($P > 0.05$, Fig. 2M). In the SBNP, the sum length of TRPV1$^+$ nerves was higher in the central cornea ($P < 0.05$, Fig. 2N) but not in the peripheral cornea ($P > 0.05$, Fig. 2N), indicating a higher proportion of TRPV1$^+$ nerves in the basal epithelium after injury. In the superficial epithelium, TRPV1$^+$ SNT density in injured corneas was similar to intact corneas ($P > 0.05$, Fig. 2O), whereas nerve density was lower in the SBNP ($P < 0.05$, Fig. 2P).

Spatial Interactions Between TRPV1$^+$ Nerves and Local Immune Cells in the Cornea

Immune Cells in the Epithelium. Given that the TRPV1$^+$ nerves represent approximately half of the total nerve population in the corneal epithelium, we next assessed their spatial interactions with resident DCs, which are known to form close contacts with corneal epithelial nerves.[36] Intraepithelial CD45$^+$ dendriform cells were found in close proximity to the TRPV1$^+$ nerve fibers (Fig. 3A, asterisk) in the SBNP (Fig. 3A, arrow). Orthogonal views of CD45$^+$ TRPV1$^+$ double immunolabeling demonstrate apparent contacts between the intraepithelial DC and TRPV1$^+$ nerve fibers in both XZ and YZ planes (Fig. 3B). To confirm the TRPV1$^+$ nerve staining, tissues were incubated overnight with the peptide control antigen, which competitively binds to the TRPV1, prior to immunostaining. Following this no immunoreactivity was observed in the corneal nerves at the level of the basal nerve plexus (Figs. 3C, D). Intraepithelial CD45$^+$ dendriform cells in proximity with the TRPV1$^+$ SBNP nerve fibers were immunopositive for CD11c eYFP and MHC-II (Figs. 3E–H), indicating that these dendriform cells are likely dendritic cells.

To assess if corneal DCs were preferentially associated with TRPV1$^+$ nerves, we quantified the percentage of intraepithelial DCs associated with βIII$^+$ TRPV1$^+$ and βIII$^+$ TRPV1$^-$ nerve fibers. In the intact corneas, the majority of intraepithelial CD45$^+$ DCs were associated with TRPV1$^+$ nerve fibers (Figs. 4A, B). This pattern was also observed in the injured corneas (Figs. 4C, D). Imaris data show physical contacts formed between the surfaces of an intraepithelial CD45$^+$ DC and βIII$^+$ TRPV1$^+$ nerve fiber in the intact (Figs. 4E–H) and injured cornea (Figs. 4I–L). In the intact corneas, the areas occupied by the DC-TRPV1$^+$ nerve fiber contacts are located along the DC dendrite (Fig. 4H, yellow colored areas). These close physical associations or neuroimmune contacts in the DC dendrites were also notable in the injured corneas (Fig. 4L, blue colored areas). Quantitative assessment of 3D image reconstructions (Supplementary Figure S1) showed a preferential contact between DC and TRPV1$^+$ axons in intact and injured corneas, as indicated by a higher number of neuroimmune contact points compared with the TRPV1$^-$ axons ($P < 0.05$, S1A, B). The number of neuroimmune contacts between DC and TRPV1$^+$ axons did not change after injury ($P > 0.05$, S1C), however, a higher degree of DC-nerve interaction, as measured by percentage overlap, was observed in the injured cornea, indicating that the DCs occupied more surfaces of the damaged TRPV1$^+$ axons ($P > 0.05$, S1D).

Next, the percentage of TRPV1$^+$ and TRPV1$^-$ nerve-associated CD45$^+$ cells was quantified in the intact and injured corneas (Figs. 4M, N), with a higher percentage of TRPV1$^+$ nerve-associated CD45$^+$ cells present in the injured group compared to the intact controls ($P < 0.05$, Fig. 4M). No difference was found in the number of TRPV1$^-$ nerve-associated DCs after the injury ($P > 0.05$, Fig. 4N).

Macrophages. In light of previous anatomical evidence of stromal macrophages in physical proximity with limbal nerve trunks in the mouse cornea (37), we sought to examine whether similar associations occurred between macrophages and TRPV1$^+$ nerves in the corneal stroma. While we observed strong TRPV1 immunopositive corneal stromal nerves, we also noted TRPV1 signals associated with CD45$^+$ stromal leukocytes in the stroma of the mouse cornea (Figs. 5B–C). These punctate cytoplasmic staining patterns in the stromal leukocytes were βIII$^-$ (Fig. 5A) and negative in peptide control antibody staining (Fig. 5D). Double immunostained CD45$^+$ TRPV1$^+$ and CD68$^+$ TRPV1$^+$ corneas demonstrated the punctate TRPV1 expression in CD45$^+$ stromal leukocytes (Fig. 5E) had partial overlap with CD68/macrosialin, a lysosomal marker associated with phagocytosis in macrophages[43,44] (Fig. 5F). Orthogonal

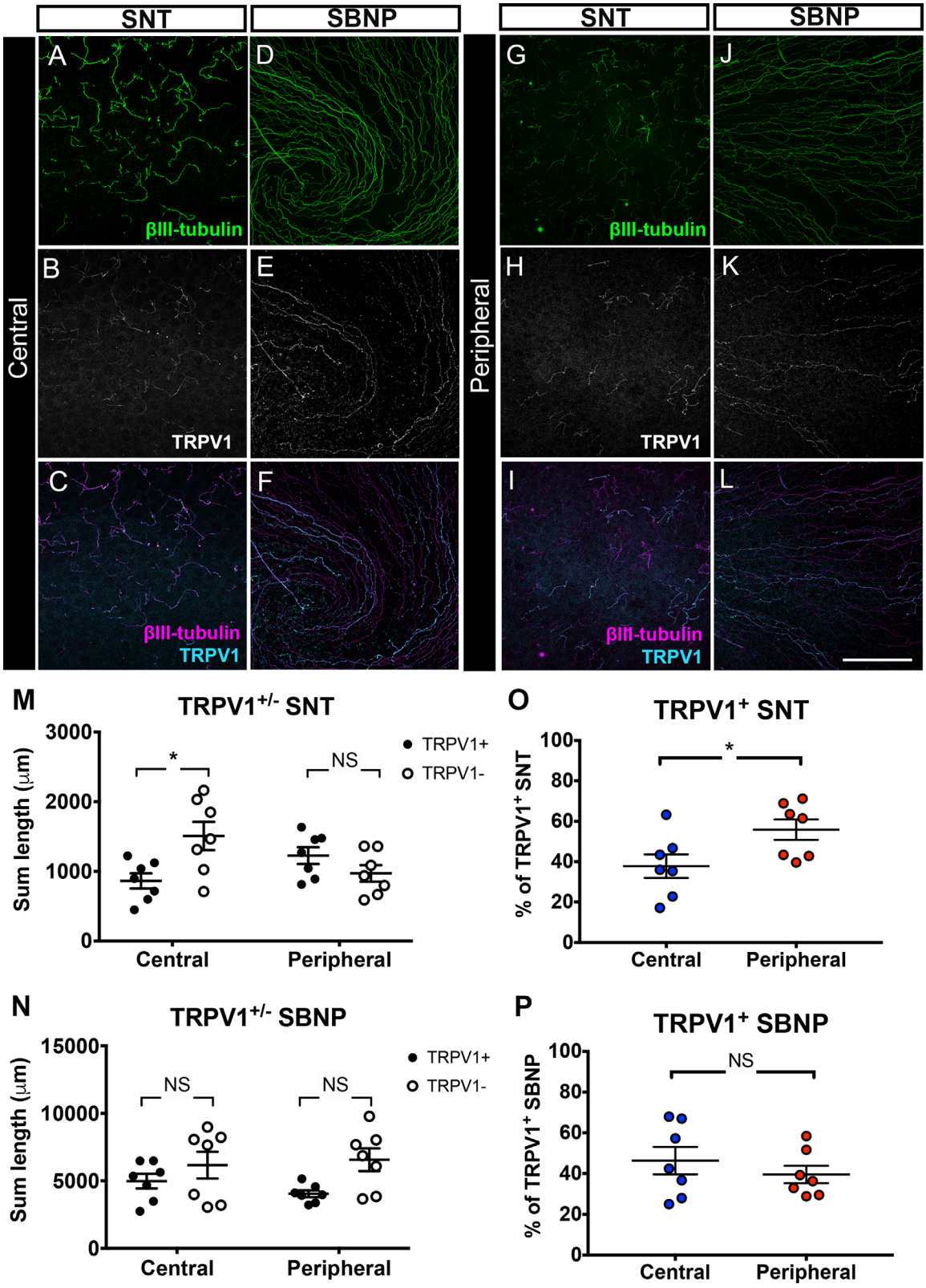

Figure 1. Topographical distribution of TRPV1$^+$ nerves in the intact mouse cornea. (**A–L**) Distribution of βIII$^+$ (**A**, **D**, **G**, and **J**) and TRPV1$^+$ (**B**, **E**, **H**, and **K**) superficial nerve terminals (SNT) and subbasal nerve plexus (SBNP) in the central (**A–F**) and peripheral corneal epithelium (**G–L**). False colored merged images demonstrate the relationship between βIII$^+$ TRPV1$^+$ (cyan) and βIII$^+$ TRPV1$^-$ (magenta) nerve fibers (**C**, **F**, **I**, and **L**). (**M–P**) The sum length of TRPV1$^+$ SNT was lower than TRPV1$^-$ SNT in the central cornea ($P < 0.05$; M) but was similar in the peripheral cornea ($P > 0.05$; M). The sum lengths of TRPV1$^+$ and TRPV1$^-$ SBNP were similar across central and peripheral cornea ($P > 0.05$, N). The percentage of TRPV1$^+$ SNT, relative to total βIII$^+$ SNTs, was higher in the peripheral cornea ($P < 0.05$; O). There were no regional differences in the percentage of TRPV1$^+$ SBNP, relative to total βIII$^+$ SBNPs ($P < 0.05$; P). Scale bars represent 100 μm for all images. Graphs are displayed as mean ± SEM, $n = 7$ per group.

Investigative Ophthalmology & Visual Science

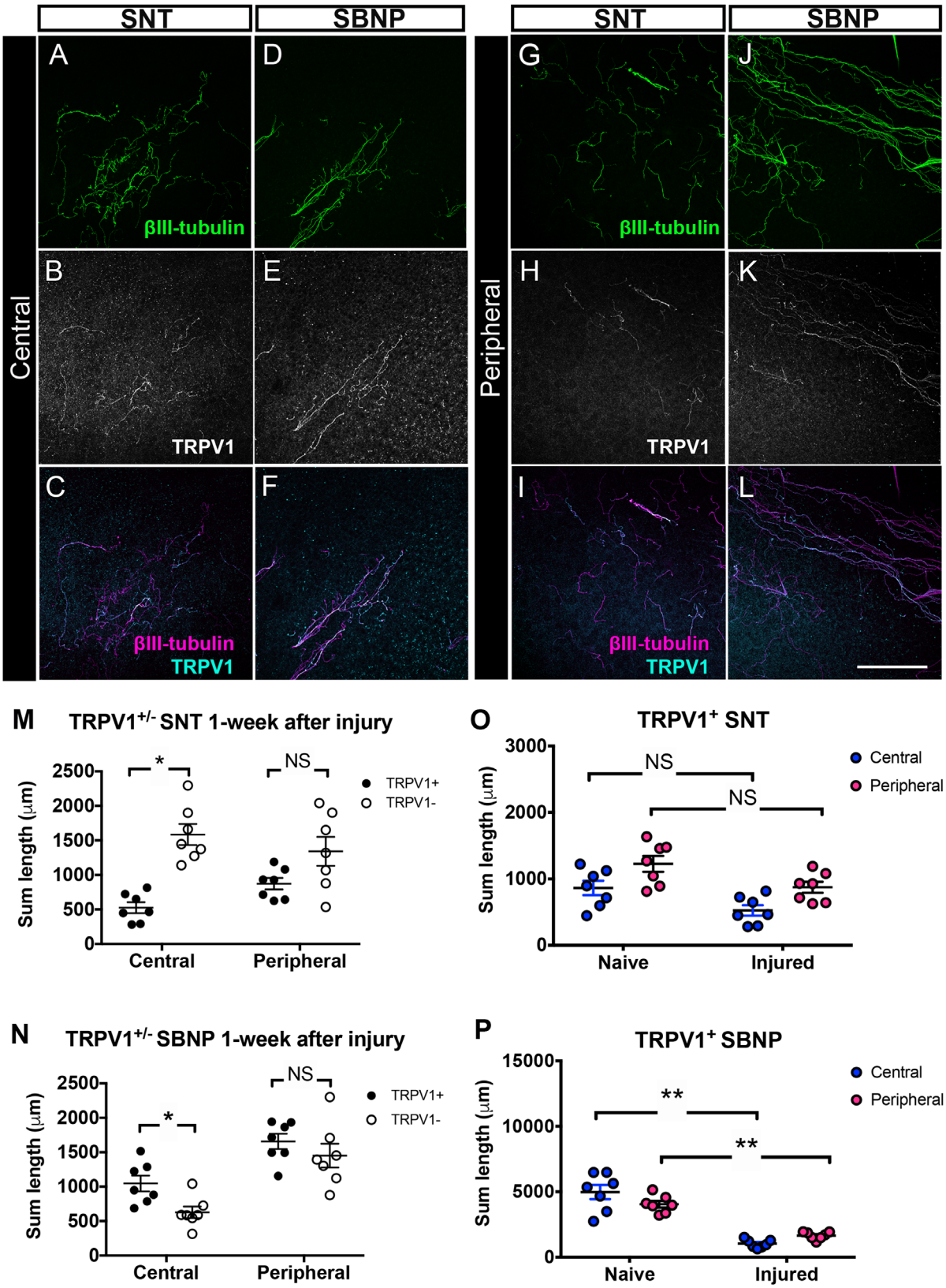

Figure 2. Recovery of TRPV1$^+$ nerves one week after a sterile epithelial abrasion (**A–L**). The distribution of βIII$^+$ TRPV1$^+$ nerves was different across the central (**A–F**) and peripheral cornea (**G–L**). (**M**, **N**) One-week post-injury, the sum length of TRPV1$^+$ SNT was lower than TRPV1$^-$ SNT in the central cornea ($P < 0.05$; M) but not in the peripheral cornea ($P > 0.05$; M). The sum length of TRPV1$^+$ SBNP was higher than TRPV1$^-$ SBNP in the central cornea ($P < 0.05$; N) but similar across the peripheral cornea ($P > 0.05$; N). (**O**) When compared to intact corneas, the sum lengths of TRPV1$^+$ SNT was similar after injury in both the central and peripheral cornea as indicated by the sum length ($P > 0.05$). (**P**) TRPV1$^+$ SBNP displayed an incomplete recovery after injury ($P < 0.05$). Scale bars represent 100 μm. Graphs are displayed as mean ± SEM with each data point representing each mouse, $n = 7$ per group.

Investigative Ophthalmology & Visual Science

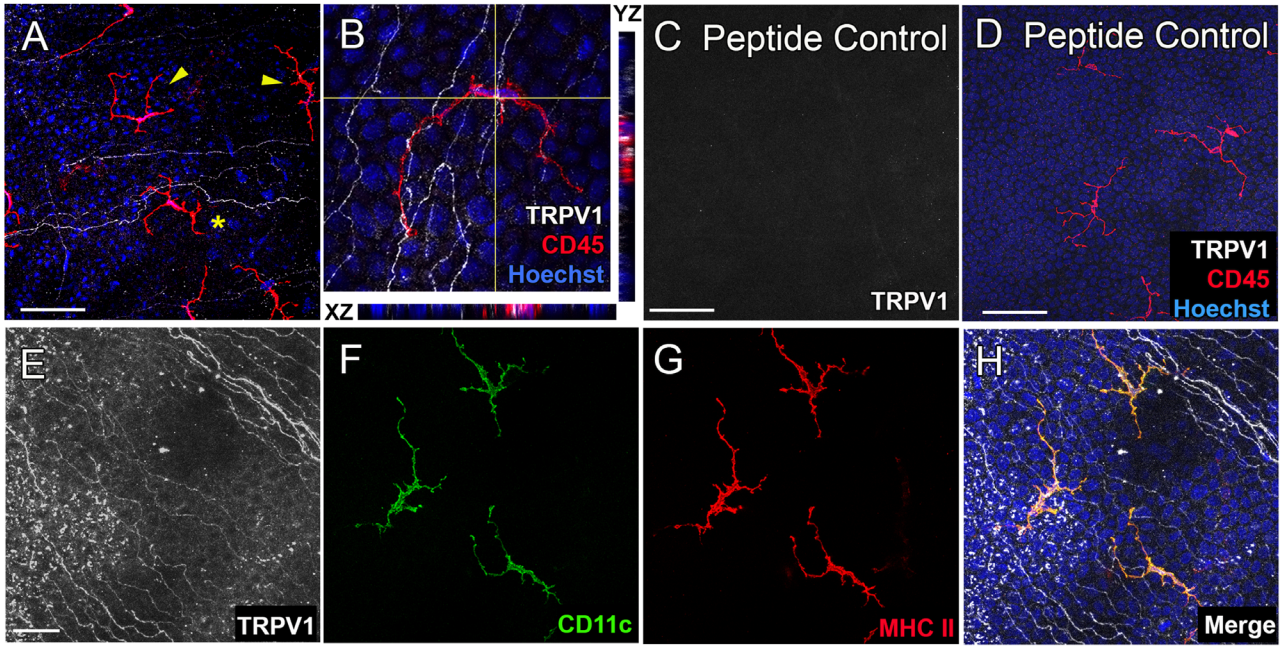

Figure 3. Epithelial TRPV1$^+$ nerves and resident dendritic cells (DCs) under steady state conditions. (**A**) Representative images from the peripheral corneal epithelium showing resident intraepithelial CD45$^+$ DCs in close proximity to TRPV1$^+$ axons (asterisk), while some DCs did not appear to associate with TRPV1$^+$ axons (arrowheads). (**B**) Orthogonal view of an intraepithelial CD45$^+$ DC highlights the contacts between the TRPV1$^+$ axons and DC in XYZ planes. (**C, D**) The absence of TRPV1 nerve staining in the peptide control validates the positive corneal nerve staining for TRPV1. (**E–H**) The resident DCs were immunopositive for CD11c and MHC class II. Scale bars represent 50 µm (**A**, **C**, **D**) and 10 µm (**E**, **F**, **G**, **H**).

views of CD45$^+$ TRPV1$^+$ and CD68$^+$ TRPV1$^+$ dual-stained corneas revealed TRPV1 expression within macrophage lysosomes (Figs. 5G, H).

We next assessed the association of βIII$^+$ TRPV1$^{+/-}$ stromal nerves with CD45$^+$ TRPV1$^{+/-}$ macrophages in the central and peripheral regions of intact (Figs. 6A, B) and injured corneas (Figs. 6C, D). TRPV1$^+$ nerves accounted for ~80% of the total stromal nerve plexus ($P > 0.05$, Fig. 6F). After the central debridement, the sum length of TRPV1$^+$ stromal nerves was similar to the sum length of TRPV1$^-$ stromal nerves ($P < 0.05$, Figs. 6G–H).

Analysis of the distribution of TRPV1 expression in CD45$^+$ macrophages showed a significantly higher abundance of CD45$^+$ TRPV1$^+$ macrophages when compared to CD45$^+$ TRPV1$^-$ macrophages in intact corneas ($P < 0.05$, Fig. 6I). The density of CD45$^+$ TRPV1$^+$ macrophages was similar in the injured central and peripheral cornea ($P > 0.05$, Fig. 6J), however, the number of CD45$^+$ TRPV1$^-$ macrophages were more abundant in injured compared to intact corneas ($P < 0.05$, Fig. 6L), indicating that the corneal injury shifted the profile of TRPV1-expressing macrophages.

Validation of TRPV1 Expression in Nerves and Immune Cells

To further validate the TRPV1 antibody specificity in corneas we examined the staining in WT and TRPV1$^{-/-}$ mice. In WT mouse corneas, TRPV1 expression was notable in the nerves and stromal macrophages (Figs. 7A, B) but was absent in TRPV1$^{-/-}$ mouse corneas (Figs. 7C, D). The positive TRPV1 reactivity in macrophage lysosomes observed in WT corneas was undetected in TRPV1$^{-/-}$ corneas (Figs. 7E–G). Punctate TRPV1 signals in the apical epithelium of TRPV1$^{-/-}$ cornea confirms that the epithelial nonneuronal signals were nonspecific to the antibody or background noise.

Discussion

This study comprehensively reports the distribution of TRPV1$^+$ nerves in the mouse cornea during steady-state conditions and following epithelial injury. The novel expression of TRPV1 by resident corneal stromal macrophages was also reported.

Topographical Distribution of TRPV1$^+$ Nerves During Steady State and Injury

Our data show that in the corneal epithelium the TRPV1$^+$ SNT and SBNP account for ~40% of the total intraepithelial nerve population with a higher degree of colabeling of the epithelial nerve terminals in the peripheral cornea, whereas TRPV1$^+$ stromal nerves account for ~80% of the total stromal nerve architecture. The present study reveals that the proportion of TRPV1$^+$ nerve fibers in the basal epithelium is higher after injury suggesting, at least at one week after injury, that the population of TRPV1$^+$ nerves might recover at a different rate to TRPV1$^-$ nerves. This idea of differential recovery of distinct nerve subsets after epithelial injury is consistent with similar reports comparing SP$^+$ and TRPM8$^+$ nerve fiber regeneration after trauma.[22,45] Interestingly, the functional responses of TRPM8$^+$ nerves was elevated after epithelial injury, suggesting an increased sensitivity of corneal neurons to cold stimuli.[45] We have previously reported that four weeks following corneal

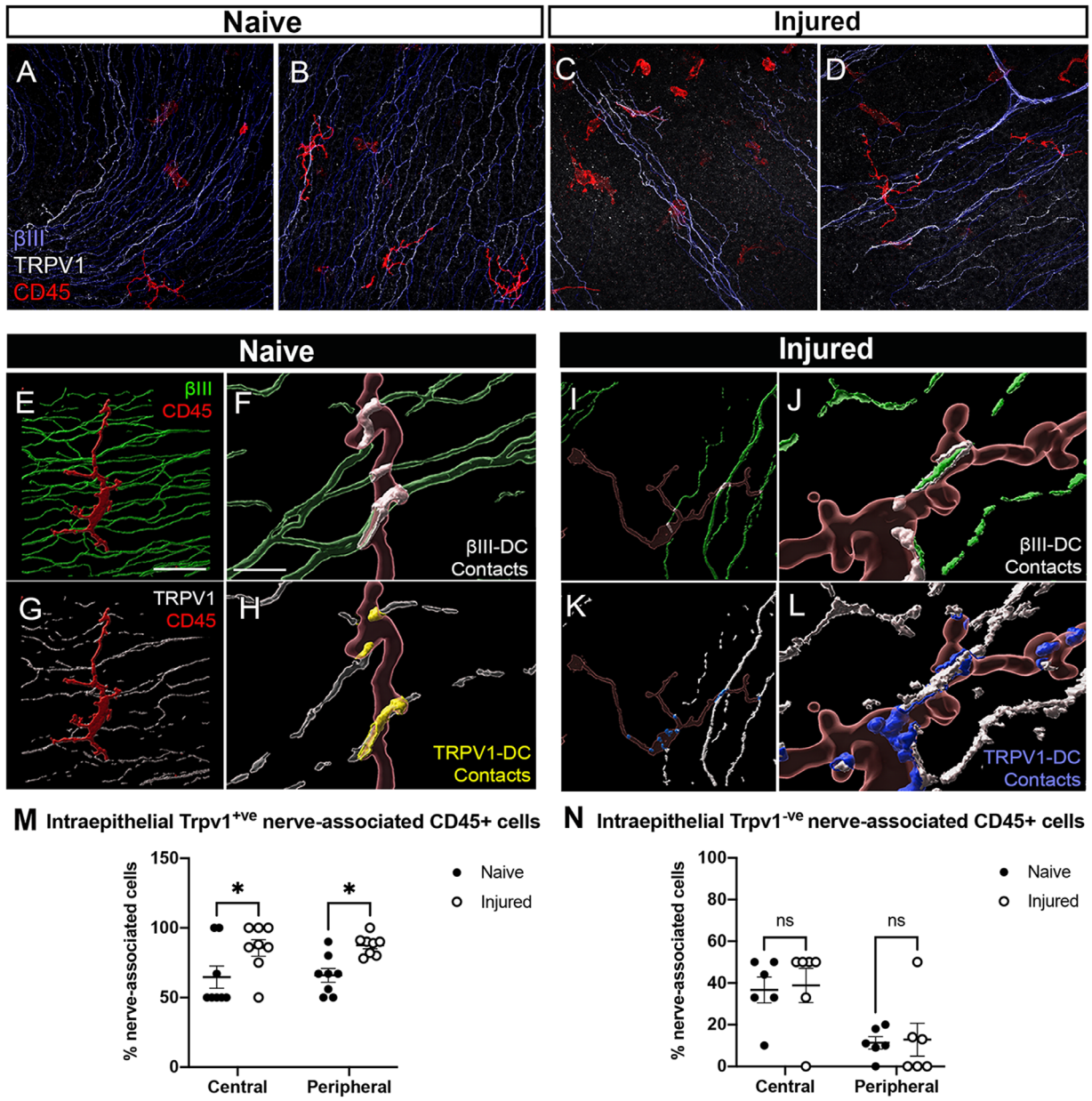

Figure 4. Intraepithelial CD45$^+$ dendriform cells in intact and injured corneas. (**A–D**) βIII, TRPV1, and CD45 staining demonstrate TRPV1$^+$ and TRPV1$^-$ nerve populations and their anatomical associations with DCs in the central and peripheral epithelium of intact (**A**, **B**) and injured corneas (**C**, **D**). (**E–L**) 3D image reconstructions show DC-nerve contacts between epithelial CD45$^+$ DCs and βIII$^+$ TRPV1$^+$ SBNP nerve axons (green: βIII; white: TRPV1). (**G–H**) DC-nerve complexes between DC and nerve axons (white area: βIII; yellow: TRPV1) were found within the DC dendrite. (**I–L**) One week after the epithelial abrasion, the degree of neuroimmune contacts between the DCs and nerve axons was similar to that observed in intact corneas (white area: βIII; blue: TRPV1) and DC dendrites. (**M, N**) The percentage of TRPV1$^+$ nerve-associated DC was significantly higher across both central and peripheral corneas in the injured group compared to the intact control corneas ($P < 0.05$), while no change occurred in the percentage of TRPV1-nerve-associated DC populations ($P > 0.05$). Scale bars represent 100 µm (**A–D**), 10 µm (**E**, **F**, **I**, **J**) and 20 µm (**G**, **H**, **K**, **L**). Graphs are displayed as mean ± SEM with each data point representing each mouse, $n = 7$ per group.

abrasion injury in mice, epithelial nerve terminal density was similar to intact corneas, but the sum length of underlying basal nerve fibers was lower, suggesting that the apically located nerve terminals recover faster than the intraepithelial nerve fibers.[39] Here, we reported a similar sum length of superficial nerve terminals, compared to intact corneas, one week after the injury. Whether this differential reestablishment of TRPV1$^+$ nerve architecture in injured corneas translates to altered function or sensitivity to noxious stimuli is unknown.

Neuroimmune Interactions Between Nociceptors and Corneal Immune Cells

The close physical relationship between corneal nerves and DCs has been reported previously in mouse[36,38] and human corneas.[46–48] Our evidence of epithelial neuroimmune interactions suggests that DCs preferentially associate with TRPV1$^+$ nerves, during both homeostasis and after injury. These data were primarily derived by quantifying the percentage of DCs in association with TRPV1$^+$ or

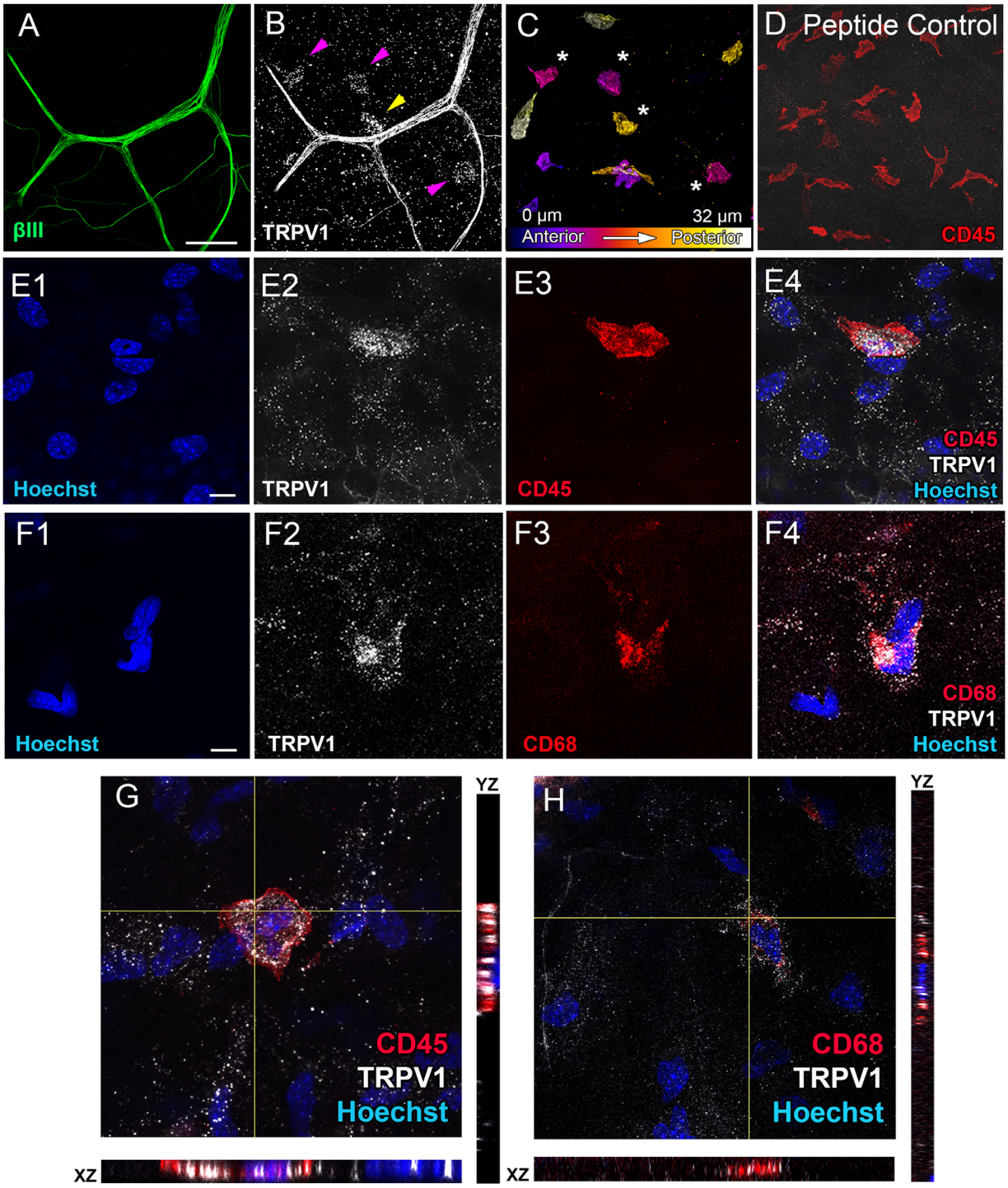

Figure 5. TRPV1 localization in nonneuronal cell bodies and their partial overlap with lysosomes of the stromal macrophages. (**A–C**) βIII$^+$ stromal nerve trunks expressed TRPV1. Intracellular TRPV1 staining was present in the macrophages that were in various depths of the stroma (color-coded depth projection, anterior: blue/purple; posterior: yellow) (**B**, arrowheads; **C**, asterisks). (**D**) Absence of TRPV1 staining in tissues treated with peptide control antigen alongside positive staining of stromal CD45$^+$ cells (red). (**E1–4**) High resolution image of TRPV1 staining within the CD45$^+$ stromal macrophages. (**F1–4**) TRPV1 partially overlapped with the macrophage intracellular compartment that expresses CD68. (**G**) Orthogonal view of a CD45$^+$ TRPV1$^+$ stromal macrophage displaying the nonneuronal TRPV1 localization in both XY and XZ planes of the z-stack. (**H**) Orthogonal view of a CD68$^+$ TRPV1$^+$ stromal macrophage shows the overlap between lysosomes and TRPV1 proteins. Scale bars represent 100 µm (**A–D**) and 10 µm (E1–4, F1–4, G, H).

TRPV1$^-$ nerve axons, a method used in clinical studies to consider corneal nerve–DC interactions using in vivo confocal microscopy.[49] Given that DCs have large field areas and several processes, and they are located within a dense plexus of nerve axons, the likelihood of DCs to be in contact with nerve axons is high. To interrogate this spatial interaction

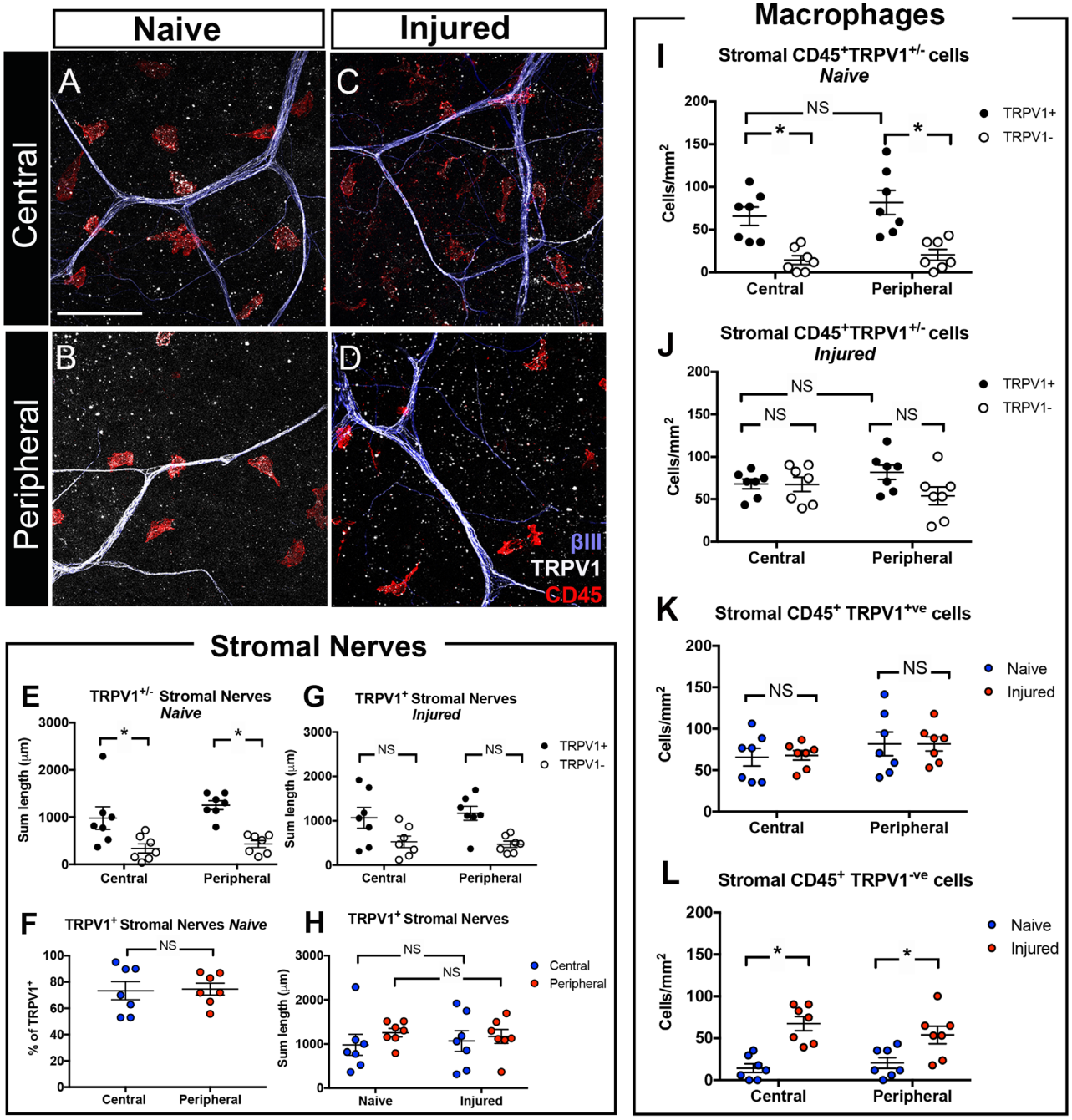

Figure 6. Stromal TRPV1$^+$ nerves and CD45$^+$ TRPV1$^+$ macrophages in intact and injured corneas. (**A–D**) Superimposed images of βIII, TRPV1, and CD45 staining demonstrate TRPV1$^+$ and TRPV1$^-$ nerves and their anatomical interaction with macrophages in central and peripheral stroma of intact (**A**, **B**) and injured corneas (**C**, **D**). (**E–H**) The sum lengths of TRPV1$^+$ stromal nerves were higher in both central and peripheral regions of the intact corneas ($P < 0.05$; E). In both regions, TRPV1$^+$ nerves account for 75% of the total sum length of stromal nerves (**F**). (**G–H**) One week after the injury, the sum lengths of TRPV1$^+$ and TRPV1$^-$ stromal nerves were similar across the different regions ($P > 0.05$) and no significant difference when compared to the intact group ($P > 0.05$) (**I–L**) CD45$^+$TRPV1$^{+/-}$ macrophage density were quantified in both groups. (**I**) Central and peripheral regions of the intact corneas had a higher density of TRPV1$^+$ macrophages ($P < 0.05$). (**J**) One week after the injury, the central and peripheral cornea showed similar number of TRPV1$^+$ and TRPV1$^-$ macrophages ($P > 0.05$). (**K**) TRPV1$^+$ macrophage density was not significantly different between intact and injured groups ($P > 0.05$). (**L**) TRPV1$^-$ macrophage density was higher after injury ($P < 0.05$). Scale bars represent 75 μm. Graphs are displayed as mean ± SEM with each data point representing each mouse, $n = 7$ per group.

further, we adopted another approach to measure the extent of overlap of the nerve and DC surfaces using Imaris. While this method has been previously reported to demonstrate spatial interactions between sensory nerves and DCs in the airway mucosa,[25] this approach, which relies on acquisition of high-resolution z-stacks with small (i.e., 0.35 μm) step sizes, is time consuming and can be subject to user bias during the manual creation of the virtual surfaces which are

Investigative Ophthalmology & Visual Science

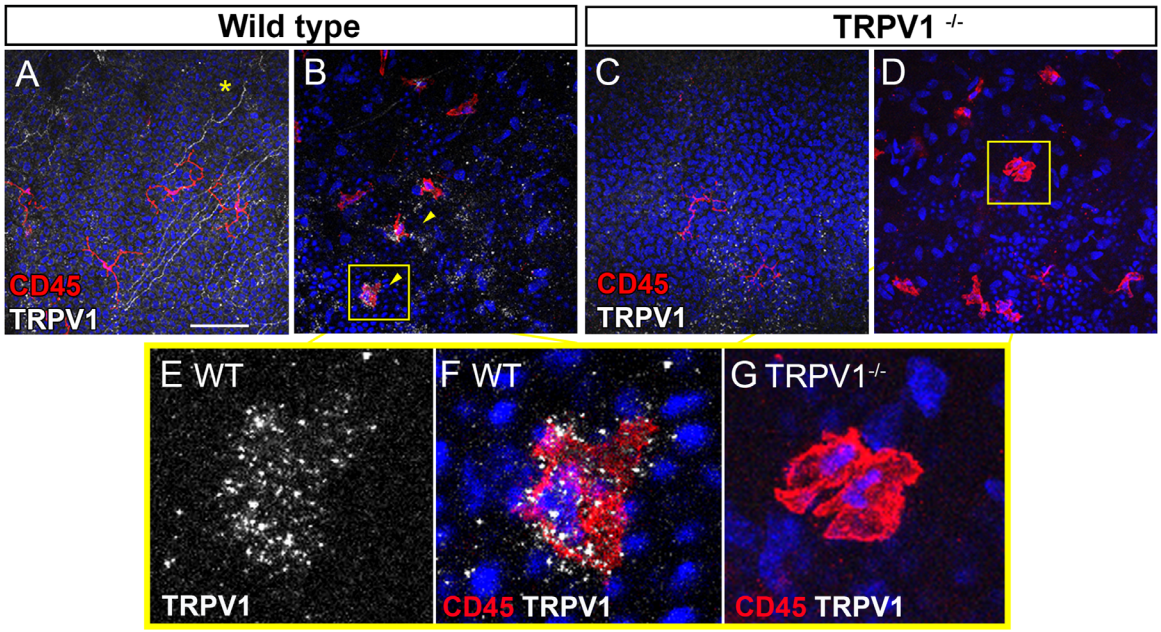

Figure 7. TRPV1 expression in wild type (WT) and TRPV1$^{-/-}$ mice. Localization of TRPV1 in corneal nerves and its intracellular localization in the stromal macrophages in wild type mouse corneas (**A, B**), and absent in the TRPV1$^{-/-}$ mouse cornea (**C, D**). The punctate staining in the epithelium was present in the TRPV1$^{-/-}$ mice, likely representing nonspecific background staining. Scale bars represent 50 µm for all images. (**E, F**) Punctate TRPV1 signals in the CD45^{+} stromal macrophages were present in the WT but absent in the TRPV1$^{-/-}$ mouse corneas (**G**).

used to quantify the degree of surface overlap. Nonetheless, our analysis suggests a preferential association of corneal epithelial DCs with TRPV1^{+} axons, when compared with TRPV1^{-} axons, in the intact and injured mouse cornea. The nature of the spatial neuroimmune interactions between the nociceptors and DCs before and after abrasion is akin to the reported interactions in the central nervous system between the TRPV1^{+} nerves and DCs in the mouse dura mater.[50] It is plausible that the direct interactions between the intraepithelial DCs and TRPV1^{+} nerve fibers may support the robust recovery of the corneal nociceptors after injury, which is concomitant with other reports on the neuroprotective role of DCs in corneal nerve support and regeneration after sterile abrasion.[36,38]

Nonneuronal TRPV1 expression has been reported in bone marrow-derived DCs[51] as well as in splenic DCs that secreted neuropeptide CGRP after exposure to a TRPV1 agonist, capsaicin.[52] In this study, we did not find direct evidence of positive TRPV1 signal within the intraepithelial MHC-II^{+} CD11c^{+} DC cells, but did consistently observe expression of TRPV1 within stromal macrophages. The intracellular localization of TRPV1 in the stromal macrophages, with the immunoreactive signal overlapping with CD68^{+} lysosomes, was an intriguing observation. Expression of TRP ion channels including TRPV1, TRPV2, TRPM2, TRPM4, and TRPM8 in immune cells has been reported in human peripheral blood mononuclear cells[53,54] and tissue resident macrophages in murine gut and lung.[35,55–57] TRPV2 and TRPM8 expression in peritoneal and alveolar macrophages are involved in the regulation of macrophage recruitment and effector functions.[35,55,56] In the CNS, TRPV1 expression was localized to mitochondria in microglia,[58] and promoted microglial migration and neuropathic pain after a chemically induced brain injury.[59] In our study, the proportion of macrophages expressing TRPV1 was lower in injured corneas, suggesting that TRPV1 expression in resident macrophages is implicated in tissue homeostasis. One explanation for our data is that local macrophages may be phagocytosing TRPV1 protein, thus contributing to maintenance of stromal nerves. These data provide a foundation for future studies to delineate the direct implications of TRPV1 on macrophage effector functions, or vice versa, in the cornea.

Conclusions

The study documented the distribution and density of corneal TRPV1^{+} nerves in the superficial and basal epithelium and stroma during steady state and after injury. The findings suggest that different subpopulations of corneal sensory nerves may be more affected by epithelial injury than others. Distinct spatial interactions between the TRPV1^{+} nerves and local immune cells provide novel insights on the neuroimmune interplay in the murine cornea.

Acknowledgments

The authors thank Yuka Okado and Shizuya Saika from Department of Ophthalmology, Wakayama Medical University for the generous gift of TRPV1 knockout mouse eyes. The authors thank the Florey Advanced Microscopy Facility at the Florey Institute of Neuroscience & Mental Health and the University of Melbourne for provision of confocal microscopes and technical advice. We thank Daniel Poole from Monash Institute of Pharmaceutical Sciences for general guidance and early discussions of the project.

Supported by National Health and Medical Research Council Project Grant (HRC; APP1126540).

HJ designed the experiments, analyzed data, and wrote the manuscript. JJI, PGM, and HRC contributed to the project

conceptual design. HRC designed the experiments and provided the project funding support. All authors contributed to revising the manuscript, and approved the final submitted version.

Diclosure: **H. Jiao,** None; **J.J. Ivanusic,** None; **P.G. McMenamin,** None; **H.R. Chinnery**, None

References

1. Belmonte C, Acosta MC, Gallar J. Neural basis of sensation in intact and injured corneas. *Exp Eye Res*. 2004;78(3):513–525.
2. Belmonte C, Aracil A, Acosta MC, Luna C, Gallar J. Nerves and sensations from the eye surface. *Ocul Surf*. 2004;2(4):248–253.
3. Reinach PS, Chen W, Mergler S. Polymodal roles of transient receptor potential channels in the control of ocular function. *Eye Vis (Lond)*. 2015;2:5.
4. Reinach PS, Mergler S, Okada Y, Saika S. Ocular transient receptor potential channel function in health and disease. *BMC Ophthalmol*. 2015;15(Suppl 1):153.
5. Belmonte C, Nichols JJ, Cox SM, et al. TFOS DEWS II pain and sensation report. *Ocul Surf*. 2017;15(3):404–437.
6. Li F, Yang W, Jiang H, et al. TRPV1 activity and substance P release are required for corneal cold nociception. *Nat Commun*. 2019;10(1):5678.
7. Okada Y, Reinach PS, Shirai K, et al. TRPV1 involvement in inflammatory tissue fibrosis in mice. *Am J Pathol*. 2011;178(6):2654–2664.
8. Okada Y, Reinach PS, Shirai K, et al. Transient receptor potential channels and corneal stromal inflammation. *Cornea*. 2015;34(Suppl 11):S136–S141.
9. Okada Y, Shirai K, Miyajima M, et al. Loss of TRPV4 function suppresses inflammatory fibrosis induced by alkali-burning mouse corneas. *PLoS One*. 2016;11(12):e0167200.
10. Nidegawa-Saitoh Y, Sumioka T, Okada Y, et al. Impaired healing of cornea incision injury in a TRPV1-deficient mouse. *Cell Tissue Res*. 2018;374(2):329–338.
11. Sumioka T, Okada Y, Reinach PS, et al. Impairment of corneal epithelial wound healing in a TRPV1-deficient mouse. *Invest Ophthalmol Vis Sci*. 2014;55(5):3295–3302.
12. Tomoyose K, Okada Y, Sumioka T, et al. Suppression of in vivo neovascularization by the loss of TRPV1 in mouse cornea. *J Ophthalmol*. 2015;2015:706404.
13. Usui-Kusumoto K, Iwanishi H, Ichikawa K, et al. Suppression of neovascularization in corneal stroma in a TRPA1-null mouse. *Exp Eye Res*. 2019;181:90–97.
14. Caterina MJ, Schumacher MA, Tominaga M, et al. The capsaicin receptor: a heat-activated ion channel in the pain pathway. *Nature*. 1997;389(6653):816–824.
15. Alamri A, Bron R, Brock JA, Ivanusic JJ. Transient receptor potential cation channel subfamily V member 1 expressing corneal sensory neurons can be subdivided into at least three subpopulations. *Front Neuroanat*. 2015;9:71.
16. Alamri AS, Wood RJ, Ivanusic JJ, Brock JA. The neurochemistry and morphology of functionally identified corneal polymodal nociceptors and cold thermoreceptors. *PLoS One*. 2018;13(3):e0195108.
17. Hiura A, Nakagawa H. Innervation of TRPV1-, PGP-, and CGRP-immunoreactive nerve fibers in the subepithelial layer of a whole mount preparation of the rat cornea. *Okajimas Folia Anat Jpn*. 2012;89(2):47–50.
18. Guo A, Vulchanova L, Wang J, Li X, Elde R. Immunocytochemical localization of the vanilloid receptor 1 (VR1): relationship to neuropeptides, the P2X3 purinoceptor and IB4 binding sites. *Eur J Neurosci*. 1999;11(3):946–958.
19. Murata Y, Masuko S. Peripheral and central distribution of TRPV1, substance P and CGRP of rat corneal neurons. *Brain Res*. 2006;1085(1):87–94.
20. Nakamura A, Hayakawa T, Kuwahara S, et al. Morphological and immunohistochemical characterization of the trigeminal ganglion neurons innervating the cornea and upper eyelid of the rat. *J Chem Neuroanat*. 2007;34(3-4):95–101.
21. Alamri AS, Brock JA, Herath CB, et al. The effects of diabetes and high-fat diet on polymodal nociceptor and cold thermoreceptor nerve terminal endings in the corneal epithelium. *Invest Ophthalmol Vis Sci*. 2019;60(1):209–217.
22. He J, Pham TL, Kakazu AH, Bazan HEP. Remodeling of substance P sensory nerves and transient receptor potential melastatin 8 (TRPM8) cold receptors after corneal experimental surgery. *Invest Ophthalmol Vis Sci*. 2019;60(7):2449–2460.
23. Parra A, Madrid R, Echevarria D, et al. Ocular surface wetness is regulated by TRPM8-dependent cold thermoreceptors of the cornea. *Nat Med*. 2010;16(12):1396–1399.
24. Hosoi J, Murphy GF, Egan CL, et al. Regulation of Langerhans cell function by nerves containing calcitonin gene-related peptide. *Nature*. 1993;363(6425):159–163.
25. Veres TZ, Rochlitzer S, Shevchenko M, et al. Spatial interactions between dendritic cells and sensory nerves in allergic airway inflammation. *Am J Respir Cell Mol Biol*. 2007;37(5):553–561.
26. Riol-Blanco L, Ordovas-Montanes J, Perro M, et al. Nociceptive sensory neurons drive interleukin-23-mediated psoriasiform skin inflammation. *Nature*. 2014;510(7503):157–161.
27. Kashem SW, Riedl MS, Yao C, et al. Nociceptive sensory fibers drive interleukin-23 production from CD301b+ dermal dendritic cells and drive protective cutaneous immunity. *Immunity*. 2015;43(3):515–526.
28. Kolter J, Kierdorf K, Henneke P. Origin and differentiation of nerve-associated macrophages. *J Immunol*. 2020;204(2):271–279.
29. Barrette B, Hebert MA, Filali M, et al. Requirement of myeloid cells for axon regeneration. *J Neurosci*. 2008;28(38):9363–9376.
30. Stoll G, Jander S, Myers RR. Degeneration and regeneration of the peripheral nervous system: from Augustus Waller's observations to neuroinflammation. *J Peripher Nerv Syst*. 2002;7(1):13–27.
31. Cattin AL, Burden JJ, Van Emmenis L, et al. Macrophage-induced blood vessels guide Schwann cell-mediated regeneration of peripheral nerves. *Cell*. 2015;162(5):1127–1139.
32. Feng J, Yang P, Mack MR, et al. Sensory TRP channels contribute differentially to skin inflammation and persistent itch. *Nat Commun*. 2017;8(1):980.
33. Kodji X, Arkless KL, Kee Z, et al. Sensory nerves mediate spontaneous behaviors in addition to inflammation in a murine model of psoriasis. *FASEB J*. 2019;33(2):1578–1594.
34. Schwartz ES, La JH, Scheff NN, et al. TRPV1 and TRPA1 antagonists prevent the transition of acute to chronic inflammation and pain in chronic pancreatitis. *J Neurosci*. 2013;33(13):5603–5611.
35. Link TM, Park U, Vonakis BM, et al. TRPV2 has a pivotal role in macrophage particle binding and phagocytosis. *Nat Immunol*. 2010;11(3):232–239.
36. Gao N, Lee P, Yu FS. Intraepithelial dendritic cells and sensory nerves are structurally associated and functional interdependent in the cornea. *Sci Rep*. 2016;6:36414.
37. Seyed-Razavi Y, Chinnery HR, McMenamin PG. A novel association between resident tissue macrophages and nerves in the peripheral stroma of the murine cornea. *Invest Ophthalmol Vis Sci*. 2014;55(3):1313–1320.
38. Gao N, Yan C, Lee P, Sun H, Yu F-S. Dendritic cell dysfunction and diabetic sensory neuropathy in the cornea. *J Clin Invest*. 2016;126(5):1998–2011.
39. Downie LE, Naranjo Golborne C, Chen M, et al. Recovery of the sub-basal nerve plexus and superficial nerve terminals

Investigative Ophthalmology & Visual Science

after corneal epithelial injury in mice. *Exp Eye Res*. 2018;171:92–100.

40. Downie LE, Choi J, Lim JK, Chinnery HR. Longitudinal changes to tight junction expression and endothelial cell integrity in a mouse model of sterile corneal inflammation. *Invest Ophthalmol Vis Sci*. 2016;57(7):3477–3484.
41. Alamri A, Bron R, Brock JA, Ivanusic JJ. Transient receptor potential cation channel subfamily V member 1 expressing corneal sensory neurons can be subdivided into at least three subpopulations. *Front Neuroanat*. 2015;9:71.
42. Meijering E, Jacob M, Sarria JC, et al. Design and validation of a tool for neurite tracing and analysis in fluorescence microscopy images. *Cytometry A*. 2004;58(2):167–176.
43. da Silva RP, Gordon S. Phagocytosis stimulates alternative glycosylation of macrosialin (mouse CD68), a macrophage-specific endosomal protein. *Biochem J*. 1999;338(Pt 3):687–694.
44. Holness CL, da Silva RP, Fawcett J, Gordon S, Simmons DL. Macrosialin, a mouse macrophage-restricted glycoprotein, is a member of the lamp/lgp family. *J Biol Chem*. 1993;268(13):9661–9666.
45. Pina R, Ugarte G, Campos M, et al. Role of TRPM8 channels in altered cold sensitivity of corneal primary sensory neurons induced by axonal damage. *J Neurosci*. 2019;39(41):8177–8192.
46. Bitirgen G, Turkmen K, Malik RA, Ozkagnici A, Zengin N. Corneal confocal microscopy detects corneal nerve damage and increased dendritic cells in Fabry disease. *Sci Rep*. 2018;8(1):12244.
47. Colorado LH, Markoulli M, Edwards K. The relationship between corneal dendritic cells, corneal nerve morphology and tear inflammatory mediators and neuropeptides in healthy individuals. *Curr Eye Res*. 2019;44(8):840–848.
48. Cruzat A, et al. Inflammation and the nervous system: the connection in the cornea in patients with infectious keratitis. *Invest Ophthalmol Vis Sci*. 2011;52(8):5136–5143.
49. Stettner M, Hinrichs L, Guthoff R, et al. Corneal confocal microscopy in chronic inflammatory demyelinating polyneuropathy. *Ann Clin Transl Neurol*. 2016;3(2):88–100.
50. Schain AJ, Melo-Carrillo A, Borsook D, et al. Activation of pial and dural macrophages and dendritic cells by cortical spreading depression. *Ann Neurol*. 2018;83(3):508–521.
51. Basu S, Srivastava P. Immunological role of neuronal receptor vanilloid receptor 1 expressed on dendritic cells. *P Natl Acad Sci USA*. 2005;102(14):5120–5125.
52. Assas BM, Wakid MH, Zakai HA, Miyan JA, Pennock JL. Transient receptor potential vanilloid 1 expression and function in splenic dendritic cells: a potential role in immune homeostasis. *Immunology*. 2016;147(3):292–304.
53. Saunders CI, Fassett RG, Geraghty DP. Up-regulation of TRPV1 in mononuclear cells of end-stage kidney disease patients increases susceptibility to N-arachidonoyldopamine (NADA)-induced cell death. *Biochim Biophys Acta*. 2009;1792(10):1019–1026.
54. Kunde DA, Yingchoncharoen J, Jurkovic S, Geraghty DP. TRPV1 mediates capsaicin-stimulated metabolic activity but not cell death or inhibition of interleukin-1β release in human THP-1 monocytes. *Toxicol Appl Pharmacol*. 2018;360:9–17.
55. Scheraga RG, Abraham S, Niese KA, et al. TRPV4 mechanosensitive ion channel regulates lipopolysaccharide-stimulated macrophage phagocytosis. *J Immunol*. 2016;196(1):428–436.
56. Khalil M, Babes A, Lakra R, et al. Transient receptor potential melastatin 8 ion channel in macrophages modulates colitis through a balance-shift in TNF-alpha and interleukin-10 production. *Mucosal Immunol*. 2016;9(6):1500–1513.
57. Yamamoto S, Shimizu S, Kiyonaka S, et al. TRPM2-mediated Ca2+influx induces chemokine production in monocytes that aggravates inflammatory neutrophil infiltration. *Nat Med*. 2008;14(7):738–747.
58. Miyake T, Shirakawa H, Nakagawa T, Kaneko S. Activation of mitochondrial transient receptor potential vanilloid 1 channel contributes to microglial migration. *Glia*. 2015;63(10):1870–1882.
59. Marrone MC, Morabito A, Giustizieri M, et al. TRPV1 channels are critical brain inflammation detectors and neuropathic pain biomarkers in mice. *Nat Commun*. 2017;8:15292.

Investigative Ophthalmology & Visual Science